Very High Energy Gain at the Neptune Inverse Free Electron Laser Experiment

P. Musumeci*, S. Ya. Tochitsky†, S. Boucher*, A. Doyuran*, R. J. England*, C. Joshi†, C. Pellegrini*, J. Ralph†, J. B. Rosenzweig*, C. Sung†, S. Tolmachev**, G. Travish*, A. Varfolomeev**, A. Varfolomeev Jr.**, T. Yarovoi** and R. Yoder*

*Neptune Laboratory Department of Physics and Astronomy. University of California, Los Angeles, CA, 90095, USA
†Department of Electrical Engineering. University of California, Los Angeles, CA, 90095, USA
**RRCKI, Moscow, Russia

Abstract. We report the observation of energy gain in excess of 20 MeV at the Inverse Free Electron Laser Accelerator experiment at the Neptune Laboratory at UCLA. A 14.5 MeV electron beam is injected in an undulator strongly tapered in period and field amplitude. The IFEL driver is a CO2 10.6 μm laser with power larger than 400 GW. The Rayleigh range of the laser, $\sim$ 1.8 cm, is much shorter than the undulator length so that the interaction is diffraction dominated. A few per cent of the injected particles are trapped in a stable accelerating bucket. Electrons with energies up to 35 MeV are measured by a magnetic spectrometer. Three-dimensional simulations, in good agreement with the measured electron energy spectrum, indicate that most of the acceleration occurs in the first 25 cm of the undulator, corresponding to an energy gradient larger than 70 MeV/m. The measured energy spectrum also indicates that higher harmonic Inverse Free Electron Laser interaction takes place in the second section of the undulator.

INTRODUCTION

Inverse Free Electron Laser (IFEL) schemes to accelerate particles have been proposed as advanced accelerators for many years [1, 2]. In a IFEL, relativistic particles are moving through an undulator magnet. A laser is propagating parallel to the beam. The undulator magnet produces a small transverse velocity (wiggling motion) in a direction parallel to the electric vector of the electromagnetic wave so that energy can be transferred between the particles and the wave. Efficient energy exchange takes place when the electron wiggling motion and the EM wave are always in the same relative phase. The electron moving on a longer curvilinear path falls behind the wave, but the phase slippage is such that its transverse velocity changes sign synchronously with the laser field (resonant condition).

Recent successful proof-of-principle IFEL experiments have shown that along with acceleration [3, 4] this scheme offers the possibility to manipulate and control the longitudinal phase space of the output beam at the laser wavelength. First among other laser accelerator schemes, the Inverse Free Electron Laser has in fact experimentally demonstrated microbunching [5], phase-dependent acceleration of electrons [6], phase locking and multi-stage acceleration [7] and control of final energy spread [8]. Up to

CP737, *Advanced Accelerator Concepts: Eleventh Workshop,*
edited by Vitaly Yakimenko

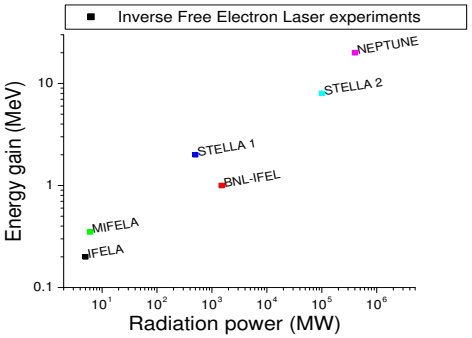

FIGURE 1. IFEL experiments around the world

now, though, only modest energy gains and gradients have been achieved in an IFEL accelerator mostly because of the relatively low peak laser power employed in the experiments carried out so far (Fig. 1).

The Inverse Free Electron Laser experiment at the Neptune laboratory at UCLA accelerated electrons from 14.5 MeV up to more than 35 MeV utilizing a CO_2 laser beam with a peak power ($\sim$ 0.4 TW), one order of magnitude greater than any other previous IFEL experiment had used. To maintain the resonant condition with the accelerating electrons, the 50 cm long undulator is strongly tapered both in period and magnetic field amplitude. An important point of the Neptune IFEL configuration is that the Rayleigh range of the laser beam is much shorter than the undulator length and the Inverse Free Electron Laser interaction is diffraction dominated.

In the following sections we describe the experimental setup, with particular emphasis on the measurements of the parameters that were more important for the outcome of the experiment. Then we present the results of the acceleration experiment and we discuss the main features of the output spectrum.

TABLE 1. Electron beam and CO_2 Laser parameters at the Neptune Laboratory

energy	14.5 MeV
charge	0.3 nC
emittance	5 mm-mrad
pulse length (rms)	3 ps
Power	400 GW
Wavelength	10.6 μ m
pulse length (rms)	100 ps
spot size	340 μ m

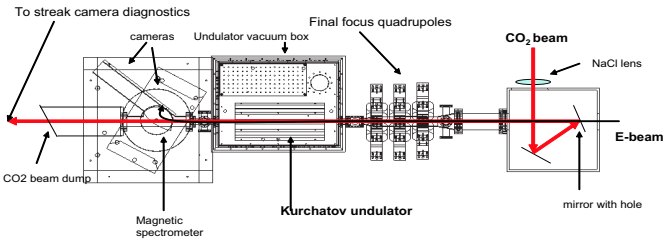

FIGURE 2. Layout of Neptune IFEL experiment

EXPERIMENTAL SETUP

In Table 1 we report the design parameters of the Inverse Free Electron Laser experiment at the Neptune Laboratory.

In Fig. 2 it is shown the experimental layout for the IFEL experiment. An electron beam of 300 pC at 14.5 MeV was delivered to the experimental region by the Neptune rf photoinjector [9]. Final focus quadrupoles with large aperture to avoid clipping of the copropagating laser beam were installed on the beamline and focused the electron beam to the nominal spot size of 150 μm rms in the middle of the undulator. A TW-class CO_2 laser system [10] was used to drive the IFEL. The laser beam is brought in vacuum through a NaCl lens that has both the function of producing the correct focusing geometry and serves as a vacuum window. The laser is made collinear to the e-beam utilizing a plane copper mirror with a hole. The beams are aligned on the probe in the midplane of the undulator with an accuracy of < 100 μm and the angular misalignment is kept below 1 mrad using the screens located before and after the undulator. After the interaction region, the e-beam is energy analyzed by the magnetic spectrometer and the laser beam is sent to the streak camera for timing measurements.

E-Beam injection energy

Because the resonant condition has to be satisfied at the beginning of the undulator in order to start the acceleration process and follow the designed orbit in the longitudinal phase space all along the interaction region, an important parameter for the accelerator is the input energy of the electron beam. The common way to measure the energy of an electron beam out of a photoinjector is to use a dispersing dipole. Usually these dipoles are compact magnets with large gaps, and any such measurement can suffer a systematic error due to the effect of the fringe-fields. This effect is of the order of magnitude of the

ratio between the dipole gap (the extent of the fringe-fields) and the dipole length and it can lead to an underestimation of the e-beam energy up to ~ 10 %.

Even after a calibration of the dipole fringe field effect, an independent check of the electron beam energy was necessary due to the strict acceptance of the accelerator to ensure the proper injection in the IFEL. This was obtained with a Cherenkov Cell threshold detector.

If a charged particle with a velocity v is moving through a medium having a refractive index n (for a given wavelength), Cherenkov radiation of that wavelength will be emitted if $v > c/n$, i.e. if $\beta n > 1$ where c is the velocity of light in vacuo and $\beta = v/c$. For gases, we can approximately take $n-1$ as being proportional to the density of gas. If the behavior of the gas is assumed to be that of an ideal gas, we can write $n-1 = kp$ where p is the pressure and k is a constant. For CO_2 gas, $n-1 = 448 \cdot 10^{-6}$ at p = 1 atm. The threshold pressure p for Cerenkov radiation is then given by $\beta \cdot (1+kp) = 1$. As the corresponding value for the total energy of the particle is very nearly proportional to $p^{-1/2}$ when $\beta \sim 1$, and as p is of the order of 1 atmosphere, the kinetic energy can be found very accurately by measuring the threshold pressure.

The energy dW per length dl of path radiated per second is given by

$$\frac{dW}{dl} = \frac{Ne^2}{c^2} \int \left(1 - \frac{1}{\beta^2 n^2}\right) \omega d\omega \tag{1}$$

where N is the number of electrons passing per second and ω is the angular frequency of the radiation. As βn is very close to unity, we can expand and write

$$\frac{dW}{dl} = \frac{Ne^2}{c^2} \int (\beta \cdot (1+kp) - 1)\, \omega d\omega \tag{2}$$

.

If a small band of frequency emitted in the visible spectrum is measured, the output above the background increases linearly with pressure for a monoenergetic beam of electrons, and the energy γ of the electrons is known from the value of the refractive index at the pressure p. In practice the transition is not so sharp. This more gradual transition is due to a number of causes, including dispersion and energy loss of the input beam in the entrance window to the detector. Three measurements on the Neptune photoinjector beam with different energy are shown in Fig. 3.

The accuracy of the Cherenkov measurement was sufficient to make sure that the injection energy was within the acceptance window of the IFEL accelerator (3%). In fact, cross-calibrating the energy measurements with the magnetic dipole and the Cherenkov detector results, the absolute energy scale for the IFEL experiment was set with a precision better than 1 %.

Kurchatov undulator

The undulator for the IFEL experiment at the Neptune Laboratory was built in collaboration with the Kurchatov Institute [11]. It is a unique magnet because of the very

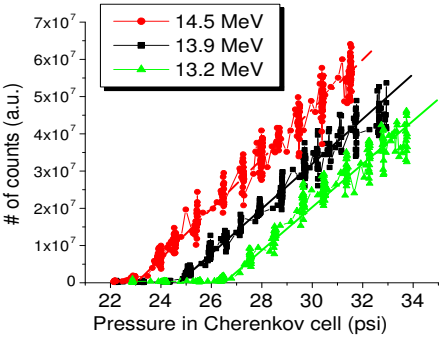

FIGURE 3. Results of electron energy measurement by Cherenkov threshold detector

strong variation of the undulator parameters (wiggling period and magnetic field amplitude) along the axis, carefully tailored to maintain the resonance condition of the IFEL interaction between the CO_2 photons and the quickly accelerating electrons.

The undulator parameters are reported in Table 2. To provide transparency for both the electron and the laser beams the undulator gap was made large, 12 mm. In order to provide synchronism in the delicate focus region [12] it was decided to build two sections and correct the field in the central region with an apposite corrector magnet. The design of the optimum tapering for the magnetic field strength and the undulator period to maximize the energy gain was based on TREDI simulations [13]. A picture of the hybrid planar permanent magnet undulator used in the experiment is shown in Fig. 4.

Accurate measurements of the magnetic field profile were obtained moving a carriage with an hall probe on the axis of the undulator. The agreement between the measured and the expected values is in every point along the axis better than 1 %.

Timing and Synchronization diagnostics

Synchronization between electrons and photons is the key for every laser accelerator with an externally injected electron beam and it is even more delicate in an IFEL

TABLE 2. KIAE undulator parameters

	initial	final
Undulator period	1.5 cm	5 cm
Magnetic field amplitude	0.16 T	0.65 T
K	0.2	2.8
Resonant energy	14.5 MeV	52 MeV

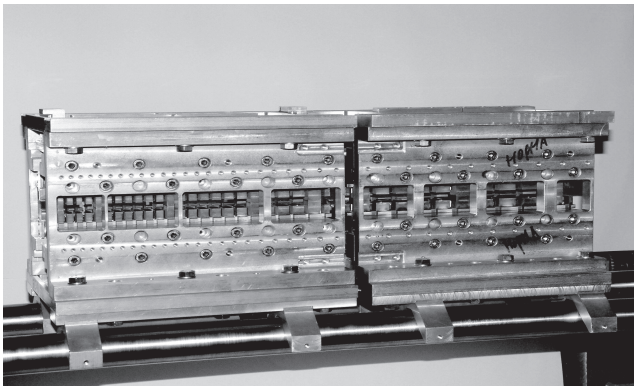

FIGURE 4. Kurchatov "double tapered" undulator

experiment. In this kind of interaction in fact, there is no resonant cavity where the accelerating wave can live independently than the laser beam. The accelerator is virtually turned on only at the time the laser pulse goes through the undulator and the ponderomotive gradient that accelerates the electrons depends on the instantaneous power felt by the electrons.

At the Neptune laboratory, the short electron pulse ($\sim$ 15 ps FWHM) and the longer CO_2 laser pulse ($\sim$ 240 ps FWHM) have been synchronized in the past with a cross-correlation method that was based on the e-beam controlled transmission of CO_2 through a Germanium sample. This technique [14] constituted the first step of the synchronization procedure also in the IFEL experiment. On the other hand, the cross-correlation measurement is conducted with the unamplified laser pulse propagating through the final triple passed, 2.5 m long multiatmosphere CO_2 amplifier with no inversion of population and has an intrinsic systematic error due to the different group velocity of the laser pulse within the inverted medium of the final amplifier in comparison with no-gain conditions. Moreover, the fluctuations in laser power (gain in the final amplifier) $\pm$ 50 % caused fluctuations in the time of arrival of $\pm$ 50 ps. This jitter was intrinsic in the laser amplification system and could not be eliminated. In order to get very accurate information on the relative timing between the electrons and the amplified pulse on each shot, we set up a new streak camera based timing diagnostics. This diagnostics allowed us to get a shot-to-shot measurement of the peak laser power as seen by the particles and it was a fundamental tool to optimize the injection time of the electrons in the IFEL accelerator.

The cathode of the streak camera is not sensible to middle infrared photon so a wavelength independent method for optical gating, based on the Optical Kerr Effect, was used to gate a long 648 nm red laser diode with the CO_2 pulse.

The Optical Kerr Effect is based on the rotation of the polarization of a relatively long probe pulse during the time when the Kerr medium is birefringent. In the diagnostic used in the IFEL experiment (Fig. 5), the birefringence is excited in the non linear medium

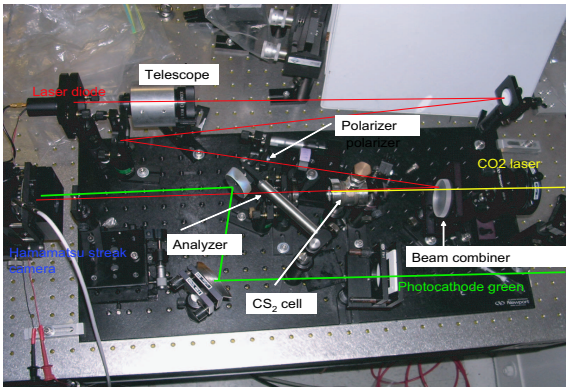

FIGURE 5. Setup for gating of the CO_2 pulse for streak camera measurements

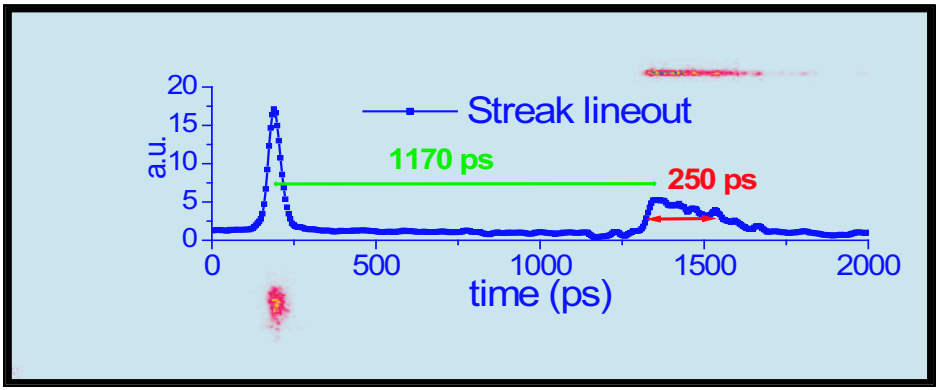

FIGURE 6. Streak camera picture of photocathode driver reference (lower-left corner) and CO2 pulse. The screen calibration gives a measurement of the laser pulse length and of the optimum delay between the reference and the CO2

by the short, intense 10.6 μm CO_2 pulse through the molecular orientation effect. The Kerr cell is placed between a polarizer and a analyzer. The function of the polarizer is to clean the polarization of the incoming laser diode pulse and to transmit only linearly polarized radiation. In the middle infrared region the best choice for the Kerr medium is CS_2 which transmit both 10.6 μm and is transparent in the visible. The gated red pulse is sent on the entrance slit of the Imacon streak camera together with a portion of the photocathode driver laser as reference of the electron beam timing.

In Fig. 6, it is shown a typical picture of the streak camera output. In the bottom left corner there is the reference green pulse from the photocathode drive laser that is representative of the electron timing. On the upper right side there is the streak of the

CO_2 pulse. The delay (1170 ps) shown in Fig. 6 corresponds to the optimal timing and it was found maximizing the output IFEL energy as a function of delay. Utilizing the streak camera diagnostics, we were able to determine for each laser shot the pulse length (and so the peak power) of the CO_2 beam and which part of the laser pulse intensity profile the electron beam sampled with an accuracy of $\pm$ 10 ps.

Laser beam delivery

The electric field that drives the IFEL interaction is the square root of the laser intensity I (I $= P/S$ where P is the laser power and S is the transverse section of the beam). The Neptune experiment was aimed to study the IFEL in the diffraction dominated configuration, that is the most direct scheme for coupling very high power laser into the undulator. For this reason, the optical geometry used in the experiment to focus and control transversely the laser beam size was of particular importance. In the original design, a 2.56 m focal length NaCl lens focused the laser in the middle of the undulator to a spot size of 340 μm with a Rayleigh range of 3.5 cm to increase as much as possible the extent of the region where the beam is more intense. The resulting peak intensity is $2 \cdot 10^{14}$ W/cm^2 in the laser focus, about two orders of magnitude more than any previous IFEL experiment used [7, 8]. Dealing with this very high laser intensities on the other hand had some disadvantages.

Experimentally, in fact, we were limited by damage threshold on the last optical elements of the CO_2 transport line and we could not increase the f-number of the optical geometry as we planned. For our typical pulse lengths of 200 ps, we observed damage on the copper mirrors for fluences above 3J/cm^2 and on the single crystal NaCl optics for fluences above 2J/cm^2. In the end, we measured a spot size of 240 μm and Rayleigh range of 1.8 cm that, respect to the original design geometry, implied a stronger variation of the beam size along the interaction region, and with the same nominal focus position at the mid-point of the undulator, a larger and less intense beam at the entrance and exit of the undulator.

To trap and accelerate particles along the design resonant orbit, the ponderomotive IFEL gradient generated by the laser electric field has to match the designed tapering gradient. If this is not the case, no trapping or acceleration are possible. Because of the differences between nominal and measured Rayleigh range, it was found out necessary to move the laser focus upstream from the nominal position to increase the intensity at the undulator entrance above the trapping threshold and start the acceleration process early in the undulator. Of course that would also cause the particles to fall out of resonance soon after the mid point of the undulator because of lack of enough ponderomotive force to sustain the acceleration along the designed orbit. It was found that the optimum position of the laser focus for the power levels available, was 2 cm (one Rayleigh range) upstream of nominal focus position.

Possible solution for the damage threshold limitation for the diffraction dominated IFEL configuration could be the use of a 5 m long focal length lens. Despite seemed simplicity, this idea was impractical because of Neptune Laboratory space available.

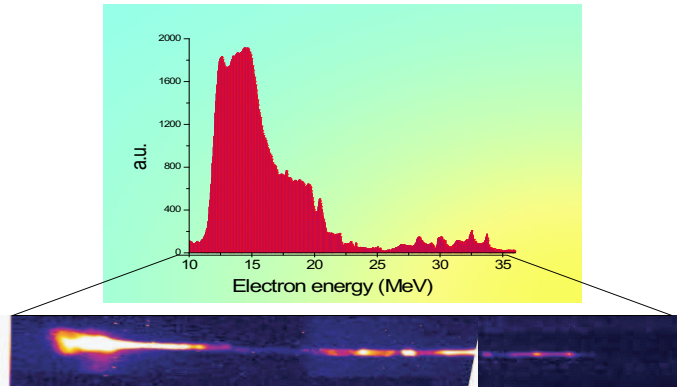

FIGURE 7. Single shot spectrum of the Inverse Free Electron Laser accelerator. More than 5 % of particles are accelerated to 35 MeV with 150 % energy gain

RESULTS

The beam at the exit of the undulator was sent into a magnetic spectrometer with a Browne and Buechner pole configuration. The Browne and Buechner geometry was chosen because it allowed a broadband energy detection capability necessary to capture in one shot the entire broad energy spectrum out of the IFEL accelerator. A factor of three in electron energy is detectable with the Neptune high energy spectrometer [15]. The dispersion varies significantly along the output slit and the resolution in energy increases roughly linearly with the energy.

The electrons were detected by a phosphorous screen observed by CCD cameras. The screen was attached to the thin mylar window at the exit slit of the spectrometer. Different neutral density filters were applied to each cameras to get unsaturated images of the output slit. A postprocessing application that takes into account the different filters and scales the horizontal axis of the images with energy, reconstructed the single shot spectrum of the electron beam out of the IFEL accelerator for each laser shot. A typical image of a dispersed electron beam is presented in Fig. 7 along with a reconstructed spectrum.

The energy spectrum shows more than 5 % of particles trapped and accelerated up to 35 MeV with a 150 % energy gain. The measured power in the CO_2 pulse for this IFEL shot was 400 GW of power and the laser was focused upstream of the nominal position by 2 cm.

The experiment was simulated using a three dimensional 4th order Runge Kutta code that solved the Lorentz equation for the particle motion in the combined fields of the undulator magnet and laser beam (`TREDI`) [16]. The simulations, once we put the correct laser intensity profile along the undulator, agree quite well with the experiment. In Fig. 8 the simulated longitudinal phase-spaces at two different distances along the undulator are shown. The histograms on the left of the graphs are the projection of

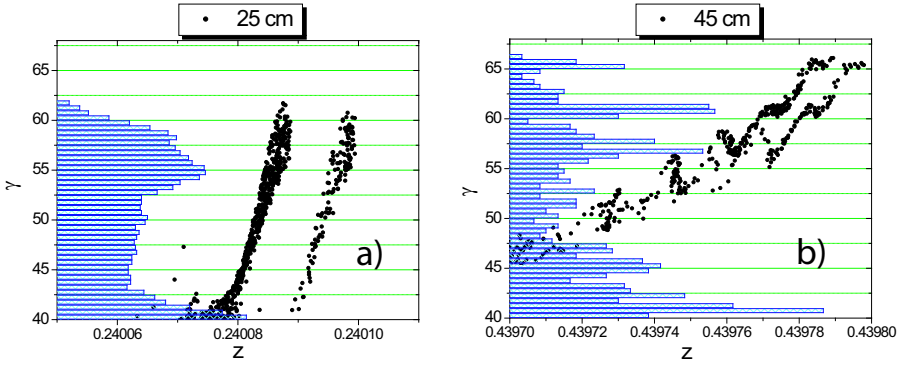

FIGURE 8. Simulations of IFEL longitudinal phase space at different points along the z axis. a) Longitudinal phase space at the undulator mid-point. The energy gain has already taken place in 25 cm. b) Energy modulation due to second harmonic interaction in the second section of the undulator. The structure in the simulated spectrum corresponds to the one in the measured spectrum

the phase-spaces on the energy axis. The simulation results allowed us to draw several conclusions.

First of all (Fig. 8a) that the IFEL acceleration mostly takes place in the first section of the undulator (first 25 cm). Few cm after the mid-point the laser intensity has decreased below the trapping threshold and the designed tapering is too strong for the particles too follow. That allows us to infer an accelerating gradient of > 70 MeV/m.

Secondly, Fig. 8b shows the structure of the high energy side of the spectrum observed in the experiment. This structure is particularly interesting because experimentally it was reproducible shot to shot, ruling out the possibility of micro-structures present in the e-beam or the laser beam. Instead, the structure is due to a different kind of IFEL interaction that takes place in the second section of the undulator.

We know that efficient energy exchange between the transverse EM wave and the particles wiggling in the undulator can only take place when the resonant condition is satisfied, and so the energy of the particles is such that in the electron's rest frame the wiggling induced by the undulator has the same frequency of the wiggling induced by the laser. On the other hand, it is known that particles of a fixed energy going through an undulator interact not only with the fundamental resonant frequency, but also with the radiation harmonics [17]. From another point of view, particles of different energy can interact with the same laser frequency, because they see the EM wave as a higher harmonic of a fundamental frequency that they are resonant with. In the Neptune IFEL experiment the particles fall out of the accelerating bucket on the resonant curve. At some point later in the undulator the particles energy is $1/\sqrt{2}$ times the resonant energy, at this point the electrons can exchange energy with the 10.6 μm photons mediated by the second harmonic IFEL interaction. This interaction is the origin of the energy modulation seen reproducibly in the output spectrum of the experiment [18].

CONCLUSIONS

We report on the observation of $>$ 20 MeV energy gain (150 %) at the Inverse Free Electron Laser experiment at the Neptune Laboratory. An energy gradient of $>$ 70 MeV/m is inferred. The fraction of self-trapped particles exceeded 5 % of the injected bunch. The acceleration gain reported is the highest obtained with an IFEL accelerator up-to-date. Self-trapping of particles in a stable accelerating bucket from a not-prebunched initial distribution was demonstrated. The effects of the laser diffraction were analyzed in the design phase and understood experimentally. Finally, higher harmonic IFEL (HH-IFEL) interaction was observed in the second section of the undulator. The HH-IFEL adds a degree of freedom (the harmonic coupling number n) in the design of magnetic systems capable of coupling lasers and electron beams. In the end, we note that the steady increase in laser power available and progress in laser technology will contribute to the continuous development of the IFEL technique that has proved once again in the Neptune experiment to be one of the most efficient ways to couple a laser beam and a particle beam.

ACKNOWLEDGMENTS

This work is supported by U.S. Dept. of Energy grant DE-FG03-92ER40693

REFERENCES

1. Palmer, R., *J. Applied Physics*, **43**, 3014 (1972).
2. Courant, E. D., Pellegrini, C., and Zakowicz, W., *Phys. Rev. A*, **32**, 2813 (1985).
3. Wernick, I., and Marshall, T. C., *Phys. Rev. A*, **46**, 3566 (1992).
4. Van Steenbergen, A., Gallardo, J., Sandweiss, J., and Fang, J. M., *Phys. Rev. Lett.*, **77**, 2690 (1996).
5. Liu, Y., et al., *Phys. Rev. Lett.*, **80**, 4418 (1998).
6. Yoder, R. B., Marshall, T. C., and Hirshfield, J. L., *Phys. Rev. Lett.*, **86**, 1765 (2001).
7. Kimura, W., et al., *Phys. Rev. Lett.*, **86**, 4041 (2001).
8. Kimura, W., et al., *Phys. Rev. Lett.*, **92**, 054801 (2004).
9. Anderson, S. G., et al., *AIP Conf. Proc.*, **569**, 487 (2000).
10. Tochitsky, S. Y., et al., *Opt. Lett.*, **24**, 1717 (1999).
11. Varfolomeev, A. A., et al., *Nucl. Instr. Meth. A*, **483**, 377–382 (2002).
12. Musumeci, P., and Pellegrini, C., *AIP Conf. Proc.*, **569**, 249–257 (2000).
13. Musumeci, P., et al., *Proc. of 2001 Particle Accelerator Conference, Chicago, Illinois*, p. 4008 (2001).
14. Tochitsky, S. Y., et al., *Phys. of Plasmas*, **11**, 2875 (2004).
15. Clayton, C. E., et al., *Proc. of 1995 Particle Accelerator Conference, Dallas, Texas*, p. 637 (1995).
16. Musumeci, P. (2004), in Ph.D. Thesis, UCLA.
17. Huang, Z., and Kim, K. J., *Phys. Rev. E*, **62**, 7295 (2000).
18. Musumeci, P., et al. (2004), to be submitted for publication.